THE ASTROPHYSICAL JOURNAL, 410:99–109, 1993 June 10

THEORETICAL MODELS FOR MASSIVE STARS IN YOUNG MAGELLANIC CLOUD STELLAR CLUSTERS

ENZO BROCATO[1] AND VITTORIO CASTELLANI[1,2]
Received 1992 May 19; accepted 1992 December 14

ABSTRACT

We extend previous evolutionary computations of intermediate-mass stars to the range of massive star models. The computations have been performed for a fine grid of metallicities covering the range $0.002 \leq Z \leq 0.02$, i.e., for a range of metallicity which appears suitable for evolving stars in young Magellanic Clouds globular clusters. Selected stellar models up to 20 $M_\odot$ have been followed from the zero-age main sequence through both the H-burning and He-burning phases till the final exhaustion of central He. The assumptions affecting the theory of massive stars are discussed, producing evidences supporting the adopted evolutionary scenario. The correlation between the star metallicity and the occurrence of blue loops during the central He burning phase is discussed, showing how star metallicity can tune the red-to-blue number ratio of He burning supergiants.

Subject headings: Magellanic Clouds — open clusters and associations: general — stars: evolution — stars: interiors

1. INTRODUCTION

According to all observational evidences, young populous stellar clusters in both Magellanic Clouds gives us the opportunity of testing the evolution of massive stars through both the H and He burning phases. The statistically significant samples of supergiants observed in those clusters have been indeed convincingly interpreted as the evidence for stars which, after the exhaustion of central hydrogen, are presently burning He in their center. As a result, one is dealing with an observational scenario which provides valuable observational constraints to be taken into account in any attempt to produce a reliable theoretical scenario.

In a recent paper (Bencivenni et al. 1991) we have recently shown that the CM distribution of stars in the young LMC cluster NGC 2004 appears in fair agreement with theoretical predictions obtained extending to selected 20 $M_\odot$ models the evolutionary scenario already presented for intermediate-mass stars (Castellani, Chieffi, & Straniero 1990, 1992). In this paper we present a grid of evolutionary sequences intended to investigate the evolutionary behavior of stars between 9 and 20 $M_\odot$. The computations have been performed for selected assumptions on the value of the star metallicity in the range $0.002 \leq Z \leq 0.02$, in order to cover a range of metallicity suitable for young Magellanic Cloud clusters. All the models have been followed from the initial zero-age main-sequence phase, through the H-burning and He-burning phases till the final exhaustion of central He.

In § 2 we present the adopted evolutionary scenario, discussing theoretical and observational evidences which are at the origin of various theoretical assumptions to be made. Section 3 is devoted to a description of the evolutionary results. A final discussion will close the paper.

2. CONSTRAINTS TO THE THEORY OF MASSIVE STARS

The evolution of massive stars is a most debated argument of stellar evolution theories. The treatment of the superadiabatic layers which develop around the H core just at the exhaustion of central H is a crucial open question concerning these structures. A large amount of the evolutionary computations given in the literature (as, e.g., the tabulation given by Maeder 1990) have been based on Schwarzschild's criterion, for which every time that $\nabla_{rad} \geq \nabla_{ad}$ convection starts mixing the stellar layers. However, an alternative approach to the treatment of convection is provided by the Ledoux criterion, for which the occurrence of a gradient in the molecular weight decreases the efficiency of convection. According to this assumption, the H-rich layers surrounding the He core of massive stars turn out to be stable against convection and no mixing sets in.

Since the pioneering paper by Stothers & Chin (1968) an abundant literature has been devoted to the argument. However, the basic evolutionary scenario was early understood: if convective shells do occur, then stars during core He burning are expected mainly at hot effective temperatures, in the blue region of the H-R diagram (see, e.g., Iben 1974). Otherwise, the star may spend a sizable portion of its lifetime at low temperatures, as a red giant or supergiant. Mass loss and core overshooting can add further complication to this simple scenario. The reader can find a careful review on this argument in the paper by Chiosi & Maeder (1986). However, one finds that a reasonable amount of mass loss does not affect drastically such an evolutionary scenario, and convective shells keep leading the star to ignite He at large effective temperature (see, e.g., Chiosi 1981).

Evolutionary consequences of the two alternative assumptions are disclosed in Figure 1, where we report the time behavior of the effective temperature of a 20 $M_\odot$ supergiant, $Y = 0.27$, $Z = 0.02$, as computed adopting either Schwarzschild or Ledoux criterion for the efficiency of convection in the shells surrounding the H exhausted stellar core. As expected, the model with mixed shells (i.e., where semiconvection is treated according to the Schwarzschild criterion) should ignite He at $\log T_e = 4.2$, spending the majority of its He burning lifetime slowly decreasing this temperature. On the contrary, the "unmixed" model rapidly reaches the Hayashi track after the overall contraction phase, burning He as a red supergiant at $\log T_e = 3.6$.

[1] Osservatorio Astronomico Collurania, I-64100 Teramo, Italy.
[2] Dipartimento di Fisica, University of Pisa, I-56100 Pisa, Italy.

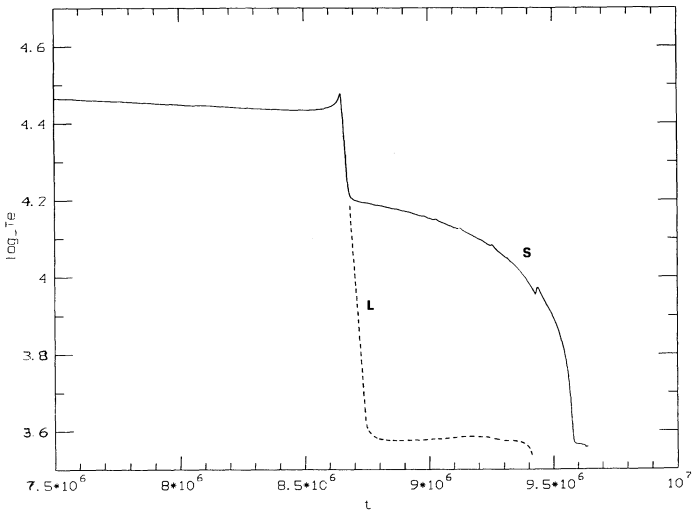

FIG. 1.—Time behavior of the effective temperature of a He burning model of a 20 $M_\odot$ star ($Y = 0.27$, $Z = 0.02$) as computed adopting Schwarzschild (S) or Ledoux (L) criterion (see text).

To discriminate between these two evolutionary behaviors, let us recall that the models presented in Figure 1 appear to be appropriate, both for luminosity and chemical composition, for He burning stars in NGC 2004, where only red supergiants are observed. Furthermore, it has been shown (Bencivenni et al. 1991) that the number of observed red supergiants appears in agreement with theoretical prescription. This simple observation suggests that Schwarzschild's procedure is running against the observational evidences, if the occurrence of core overshooting is neglected as in our computations. However, when discussing the case of NGC 2004, we found that the prescriptions of stellar evolution with negligible amount of overshooting are—at least—not contradicted by observational evidences. Similar results have been recently presented by Stothers (1991) discussing observational tests for overshooting.

According to such an evidence, we will present in the next section a grid of evolutionary models computed under the "canonical" assumptions of no overshooting, no mass loss, and adopting the Ledoux criterion for the treatment of semiconvective shells.

3. EVOLUTIONARY RESULTS

As in previous papers, evolutionary computations have been performed on the basis of FRANEC evolutionary code, whose main features have been already described (see Castellani et al. 1992, and references therein). One has to notice that, as in previous computations, we adopted radiative opacities from the Los Alamos Opacity Library (LAOL). As is well-known, such evaluations have been recently improved by the Livermore group (OPAL: Iglesias & Roger 1991a, b; Roger & Iglesias 1992), including, in particular, the contribution of many more metal lines. However, one finds that these new evaluations do not allow a meaningful coverage of the evolutionary phases we will deal with, since neither opacity values for temperature larger than $T = 10^8$ K nor for carbon and oxygen mixtures are till the present available. As a consequence, to cover the phase of He burning one should necessarily rely on LAOL tables.

Facing such a situation, and waiting for more complete tables, we are reluctant in trusting in "mixed opacities" as obtained by rather arbitrarily merging OPAL to LAOL opacities. Thus we decided to keep LAOL opacity throughout all our evolutionary computations, in order to rely on a homogeneous set of values. Such a decision has been further supported by numerical experiments, producing the evidence that the larger differences between evolutionary computations based either on OPAL or LAOL opacities can be accounted for by a moderate decrease of the nominal value of metallicity in LAOL opacities (Cassisi, Castellani, & Straniero 1993). This is because the major difference between the two tables is just the increased contribution of metals to the opacity. On this basis, we present our evolutionary scenario for massive stars, bearing in mind that the metallicity scale we are dealing with will be probably decreased by 10%–20% when improved opacity tables become available.

We choose $M \sim 20\ M_\odot$ as an upper mass limit for our computations in order to avoid the range of very massive stars where mass loss could play a critical role, remaining in a range of stellar masses which should be only scarcely affected by any reasonable amount of mass loss (Weiss 1989). In any case, we present the evolutionary scenario as a reference frame, leaving to future observations of young stellar clusters the task of disclosing if, and how, the present theory needs to be modified.

Model details are presented in Table 1: columns give, in order, model number, the log of the age (yr), the central abundance of H and of He (after H-exhaustion), the log of luminosity ($L_\odot$), the log of effective temperature, the log of central temperature, the log of central density, the mass of the convective core, the mass of the helium core, the mass of the carbon-oxygen core, the border of the convective envelope, the total luminosity produced by p-p (L_{pp}), CNO cycle (L_{cno}), 3α reactions ($L_{3\alpha}$) and gravitation (L_{gr}) in units of the surface luminosity. Solar units are used for the masses.

Figures 2–7 show the evolutionary paths in the H-R diagram of selected models for $Z = 0.02$, 0.01, 0.006, 0.004, 0.003, and 0.002. As disclosed by these figures, the fine grid of low Z-values has been adopted to follow with sufficient details the modifications with Z of the evolutionary lines. The amount of original He has been fixed at $Y = 0.27$ for the first three metallicity values, and at $Y = 0.25$ for the further three lower metallicities. This variation is intended to approach the expected variation of Y with Z, taking into account that the precise value of Y plays a minor role in the evolutionary characteristics of our models.

From inspection of the above quoted figures, one recognizes evolutionary features in agreement with the evolutionary scenario early discussed by Alcock & Paczyński (1978) for less massive stars. At the larger metallicities, all stars begin burning He on their Hayashi track. On the contrary, for the lower metallicities, He burning starts just when the star is moving toward the Hayashi track, pushing the star again toward large effective temperatures. Such a behavior is the result of adopting the Ledoux criterion in the treatment of semiconvection. Adopting Schwarzschild's criterion we found that, varying Y between $Y = 0.20$ and $Y = 0.28$ and/or lowering Z down to $Z = 0.002$, all models ignite He at large effective temperatures moving toward the Hayashi track only at the exhaustion of central He.

Figures 2–7 disclose other features worthy of discussion. At the larger metallicities, i.e., for $Z \geq 0.006$, blue loops during the He burning phase occur only for stars with $M < 12\ M_\odot$. As a consequence, one does not expect blue supergiants at luminosity larger than $\log L/L_\odot \approx 4.5$, that is at $M_{bol} \approx -7$. This is

TABLE 1

PROPERTIES OF MASSIVE EVOLUTIONARY TRACKS

20M -- Y=0.27 -- Z=0.02

nmd	logt	H/He	logL	logTe	logTc	logρc	Mcc	Mc_He	M_CO	Mce	Lpp	Lcno	L3α	Lgr
6	4.19127035	0.71	4.621	4.543	7.549	0.667	9.05505	0.00000	0.00000	0.000	0.002	0.998	0.000	0.000
39	6.33911753	0.59	4.686	4.529	7.544	0.620	8.28112	0.00000	0.00000	0.000	0.001	0.999	0.000	0.000
69	6.58836508	0.48	4.746	4.519	7.552	0.619	7.50718	0.00000	0.00000	0.000	0.000	1.003	0.000	-0.003
96	6.71610022	0.37	4.800	4.506	7.564	0.632	6.73324	0.00000	0.00000	8.591	0.000	1.003	0.000	-0.003
120	6.79573059	0.26	4.849	4.488	7.578	0.660	6.03670	0.00000	0.00000	8.591	0.000	1.004	0.000	-0.004
144	6.84517193	0.15	4.888	4.468	7.595	0.705	5.31436	0.00000	0.00000	8.281	0.000	1.004	0.000	-0.004
198	6.88163471	0.05	4.924	4.447	7.628	0.802	4.69521	0.00000	0.00000	8.281	0.000	1.003	0.000	-0.003
390	6.89616632	0.00	4.960	4.472	7.727	1.110	4.08638	0.00000	0.00000	8.281	0.000	0.899	0.000	0.101
438	6.89658022	0.98	4.981	4.488	7.806	1.430	0.00000	4.82936	0.00000	5.830	0.000	0.735	0.000	0.265
456	6.89681387	0.98	4.963	4.460	7.867	1.786	0.00000	4.64362	0.00000	5.129	0.000	1.204	0.000	-0.204
468	6.89698076	0.98	4.978	4.428	7.914	2.010	0.00000	4.64362	0.00000	5.108	0.000	1.186	0.000	-0.186
477	6.89710855	0.98	4.988	4.402	7.951	2.172	0.00000	4.64362	0.00000	5.108	0.000	1.167	0.000	-0.167
486	6.89723444	0.98	4.995	4.376	7.990	2.332	0.00000	4.54043	0.00000	5.108	0.000	1.151	0.000	-0.151
495	6.89735460	0.98	4.998	4.349	8.030	2.483	0.00000	4.54043	0.00000	5.149	0.000	1.137	0.000	-0.137
504	6.89746761	0.98	4.998	4.321	8.071	2.619	0.00000	4.54043	0.00000	5.172	0.000	1.121	0.000	-0.121
513	6.89756870	0.98	4.997	4.293	8.107	2.739	0.00000	4.64362	0.00000	5.392	0.000	1.103	0.000	-0.103
522	6.89766121	0.98	4.995	4.265	8.141	2.843	0.00000	4.64362	0.00000	5.495	0.000	1.088	0.001	-0.089
531	6.89773417	0.98	4.991	4.240	8.170	2.916	0.09287	4.64362	0.00000	5.598	0.000	1.073	0.015	-0.087
552	6.89781570	0.98	4.985	4.208	8.198	2.969	0.57787	4.64362	0.00000	5.753	0.000	1.041	0.123	-0.164
561	6.89787722	0.98	4.979	4.182	8.210	2.977	1.11447	4.65652	0.00000	6.114	0.000	1.015	0.255	-0.269
570	6.89794111	0.98	4.972	4.153	8.215	2.973	1.44468	4.74681	0.00000	7.352	0.000	1.007	0.320	-0.328
579	6.89799929	0.97	4.965	4.123	8.219	2.969	1.69234	4.74681	0.00000	7.314	0.000	1.015	0.332	-0.347
588	6.89805031	0.97	4.958	4.093	8.222	2.969	1.85745	4.74681	0.00000	8.281	0.000	1.032	0.318	-0.350
597	6.89809561	0.97	4.951	4.062	8.224	2.970	1.94000	4.75713	0.00000	8.281	0.000	1.047	0.313	-0.360
606	6.89813614	0.97	4.944	4.030	8.226	2.971	1.94000	4.82936	0.00000	8.281	0.000	1.060	0.318	-0.378
615	6.89817142	0.97	4.938	3.999	8.228	2.974	2.02255	4.82936	0.00000	8.281	0.000	1.071	0.353	-0.424
624	6.89820385	0.97	4.931	3.966	8.229	2.975	2.02255	4.82936	0.00000	8.281	0.000	1.082	0.334	-0.417
633	6.89823246	0.97	4.924	3.932	8.231	2.977	2.10511	4.82936	0.00000	8.281	0.000	1.095	0.396	-0.490
642	6.89825678	0.97	4.917	3.901	8.231	2.976	2.10511	4.82936	0.00000	10.397	0.000	1.103	0.370	-0.473
651	6.89827967	0.97	4.909	3.868	8.232	2.977	2.10511	4.82936	0.00000	8.242	0.000	1.119	0.366	-0.485
660	6.89829922	0.97	4.902	3.835	8.232	2.977	2.18766	4.82936	0.00000	8.242	0.000	1.128	0.431	-0.559
669	6.89831829	0.97	4.892	3.801	8.232	2.975	2.18766	4.82936	0.00000	11.403	0.000	1.146	0.408	-0.554
678	6.89833498	0.97	4.880	3.765	8.233	2.975	2.18766	4.83968	0.00000	8.242	0.000	1.177	0.407	-0.584
687	6.89834976	0.97	4.866	3.730	8.233	2.976	2.18766	4.83968	0.00000	8.242	0.000	1.212	0.415	-0.627
696	6.89836311	0.97	4.848	3.696	8.233	2.976	2.18766	4.85000	0.00000	8.242	0.000	1.257	0.430	-0.686
705	6.89837503	0.97	4.826	3.664	8.234	2.976	2.18766	4.85000	0.00000	8.242	0.000	1.318	0.453	-0.771
714	6.89838552	0.97	4.797	3.638	8.234	2.976	2.18766	4.85000	0.00000	8.242	0.000	1.399	0.486	-0.884
735	6.89840412	0.97	4.739	3.612	8.234	2.974	2.27021	4.86032	0.00000	19.297	0.000	1.568	0.622	-1.189
777	6.89843225	0.97	4.805	3.586	8.234	2.973	2.27021	4.86032	0.00000	10.268	0.000	1.327	0.498	-0.825
795	6.89844275	0.97	4.921	3.574	8.234	2.973	2.27021	4.87064	0.00000	8.146	0.000	1.011	0.377	-0.388
834	6.89847088	0.96	5.026	3.564	8.235	2.974	2.27021	4.87064	0.00000	7.265	0.000	0.792	0.294	-0.086
1014	6.90295696	0.85	5.065	3.561	8.247	2.939	2.76553	5.43045	0.00000	6.941	0.000	0.646	0.353	0.001
1074	6.90763760	0.74	5.046	3.563	8.257	2.929	3.09574	5.72713	0.00000	7.111	0.000	0.565	0.438	-0.003
1107	6.91183710	0.63	5.026	3.565	8.267	2.932	3.34340	5.92061	0.00000	7.323	0.000	0.486	0.520	-0.005
1140	6.91574621	0.53	5.008	3.567	8.277	2.941	3.50851	6.04960	0.00000	7.556	0.000	0.410	0.597	-0.006
1179	6.92023563	0.42	4.992	3.569	8.290	2.958	3.70973	6.19149	0.00000	7.875	0.000	0.327	0.681	-0.007
1227	6.92509413	0.31	4.983	3.570	8.304	2.983	3.86452	6.26888	0.00000	8.184	0.000	0.250	0.758	-0.007
1281	6.92932844	0.21	4.981	3.571	8.321	3.020	3.98835	6.32693	0.00000	8.300	0.000	0.194	0.814	-0.007
1380	6.93471479	0.10	4.991	3.569	8.350	3.092	3.96771	6.38497	0.00000	8.107	0.000	0.147	0.856	-0.003
1686	6.93986988	0.00	5.051	3.563	8.442	3.365	3.88516	6.44302	0.00000	7.309	0.000	0.189	0.720	0.094
1983	6.94042015	0.00	5.152	3.553	8.579	3.809	0.00000	6.45269	4.17926	6.875	0.000	0.272	0.200	0.546

not the case only in a narrow range of metallicity, i.e., for $0.002 < Z < 0.006$, connecting the "high metallicity domain" to the "low metallicity domain," where massive stars can develop a blue loop during the central He burning phase. For even lower metallicities ($Z \leq 0.002$) all stars burn He as blue supergiants. Figure 8 shows the behavior with time of the effective temperature of a 20 $M_\odot$ model computed under the labeled assumptions on the star metallicity. One finds the interesting evidence that stars making the blue loop are just shifting from a "red-state" to a "blue-state," quickly traveling the H-R diagram moving from one state to the other. As a consequence, two clumps of stars are expected, respectively, as red and blue supergiants.

It is obviously interesting to notice that this is precisely what is observed in the SMC cluster NGC 330 (Carney, Janes, & Flower 1985; Cayrel 1988). One should note that such a feature is not accounted for by models based on the Schwarzschild criterion, even including overshooting and mass loss as presented by Maeder (1990, see his Figs. 1 and 2 which should cover the range of metallicity appropriate for NGC 330). However, further investigations about NGC 330, producing complete and statistically significant samples of data, are

TABLE 1—*Continued*

20M -- Y=0.27 -- Z=0.01

nmd	logt	H/He	logL	logTe	logTc	logρc	Mcc	Mc_He	M_CO	Mce	Lpp	Lcno	L3α	Lgr
3	0.22470520	0.72	4.618	4.515	7.486	0.485	9.44202	0.00000	0.00000	0.000	0.000	1.000	0.000	0.000
42	3.98620582	0.72	4.663	4.545	7.535	0.639	6.26888	0.00000	0.00000	0.000	0.001	0.332	0.000	0.666
105	6.29092455	0.62	4.683	4.545	7.556	0.666	8.43590	0.00000	0.00000	0.000	0.001	1.002	0.000	-0.003
132	6.54621601	0.52	4.738	4.537	7.564	0.665	7.81676	0.00000	0.00000	0.000	0.001	1.002	0.000	-0.003
159	6.68982601	0.41	4.792	4.526	7.576	0.677	7.04282	0.00000	0.00000	0.000	0.000	1.003	0.000	-0.003
183	6.77673340	0.30	4.840	4.511	7.589	0.700	6.26888	0.00000	0.00000	8.900	0.000	1.003	0.000	-0.004
204	6.83208847	0.20	4.881	4.493	7.605	0.737	5.52074	0.00000	0.00000	8.900	0.000	1.004	0.000	-0.004
234	6.86838102	0.10	4.913	4.475	7.626	0.796	5.07702	0.00000	0.00000	8.900	0.000	1.004	0.000	-0.004
387	6.89778042	0.00	4.955	4.477	7.711	1.055	4.28245	0.00000	0.00000	8.900	0.000	0.973	0.000	0.027
498	6.89911985	0.99	4.984	4.505	7.816	1.447	0.18574	4.82936	0.00000	7.817	0.000	0.646	0.000	0.354
519	6.89939690	0.99	4.971	4.473	7.888	1.856	0.00000	4.64362	0.00000	5.087	0.000	1.198	0.000	-0.198
531	6.89957333	0.99	4.989	4.442	7.934	2.080	0.00000	4.64362	0.00000	5.087	0.000	1.173	0.000	-0.173
543	6.89974976	0.99	5.002	4.410	7.984	2.297	0.00000	4.54043	0.00000	5.067	0.000	1.150	0.000	-0.150
552	6.89987803	0.99	5.008	4.384	8.024	2.453	0.00000	4.54043	0.00000	5.046	0.000	1.136	0.000	-0.136
561	6.90000486	0.99	5.011	4.357	8.066	2.602	0.00000	4.54043	0.00000	5.046	0.000	1.118	0.000	-0.118
570	6.90012217	0.99	5.012	4.330	8.107	2.736	0.00000	4.54043	0.00000	5.172	0.000	1.098	0.000	-0.098
579	6.90022802	0.99	5.013	4.302	8.144	2.853	0.00000	4.54043	0.00000	5.392	0.000	1.075	0.001	-0.076
591	6.90032339	0.99	5.012	4.275	8.179	2.944	0.16511	4.64362	0.00000	5.495	0.000	1.047	0.019	-0.066
609	6.90040159	0.99	5.010	4.249	8.205	2.991	0.65011	4.64362	0.00000	5.701	0.000	1.013	0.112	-0.125
618	6.90047503	0.99	5.008	4.223	8.218	3.001	1.11447	4.64362	0.00000	5.805	0.000	0.983	0.236	-0.219
627	6.90055370	0.98	5.005	4.194	8.225	3.000	1.52723	4.66941	0.00000	6.230	0.000	0.968	0.287	-0.256
636	6.90062618	0.98	5.000	4.165	8.228	2.997	1.77489	4.74681	0.00000	7.159	0.000	0.972	0.309	-0.281
645	6.90069008	0.98	4.997	4.135	8.231	2.994	1.94000	4.74681	0.00000	7.507	0.000	0.972	0.327	-0.298
654	6.90074921	0.98	4.994	4.104	8.232	2.991	2.02255	4.74681	0.00000	7.468	0.000	0.974	0.319	-0.292
663	6.90080261	0.98	4.990	4.073	8.233	2.988	2.10511	4.76745	0.00000	8.126	0.000	0.976	0.327	-0.303
672	6.90085125	0.98	4.986	4.041	8.233	2.985	2.18766	4.82936	0.00000	8.900	0.000	0.980	0.350	-0.330
681	6.90089512	0.98	4.982	4.008	8.234	2.983	2.18766	4.82936	0.00000	8.900	0.000	0.982	0.325	-0.307
690	6.90093422	0.98	4.979	3.974	8.234	2.982	2.18766	4.82936	0.00000	8.900	0.000	0.985	0.326	-0.310
699	6.90096998	0.97	4.976	3.938	8.234	2.979	2.27021	4.82936	0.00000	8.900	0.000	0.980	0.344	-0.324
708	6.90100288	0.97	4.973	3.903	8.234	2.978	2.27021	4.82936	0.00000	0.000	0.000	0.983	0.333	-0.315
717	6.90103340	0.97	4.969	3.868	8.234	2.977	2.27021	4.83968	0.00000	9.674	0.000	0.985	0.328	-0.313
726	6.90106058	0.97	4.963	3.832	8.235	2.976	2.27021	4.85000	0.00000	8.900	0.000	0.994	0.338	-0.332
735	6.90108538	0.97	4.956	3.796	8.234	2.975	2.27021	4.85000	0.00000	8.900	0.000	1.003	0.340	-0.343
741	6.90110064	0.97	4.950	3.771	8.235	2.975	2.27021	4.85000	0.00000	11.093	0.000	1.013	0.345	-0.358
750	6.90112162	0.97	4.937	3.734	8.235	2.974	2.35277	4.86032	0.00000	10.061	0.000	1.034	0.395	-0.429
759	6.90114021	0.97	4.921	3.698	8.234	2.973	2.35277	4.86032	0.00000	8.862	0.000	1.066	0.386	-0.451
768	6.90115643	0.97	4.899	3.666	8.234	2.972	2.35277	4.87064	0.00000	8.862	0.000	1.116	0.397	-0.513
780	6.90117407	0.97	4.864	3.638	8.234	2.972	2.35277	4.87064	0.00000	8.862	0.000	1.203	0.427	-0.630
810	6.90120649	0.97	4.819	3.613	8.235	2.972	2.35277	4.88096	0.00000	17.078	0.000	1.311	0.471	-0.782
843	6.90123367	0.97	4.932	3.596	8.235	2.971	2.35277	4.88096	0.00000	9.636	0.000	0.996	0.366	-0.362
876	6.90127087	0.97	5.036	3.586	8.235	2.971	2.35277	4.89128	0.00000	7.991	0.000	0.780	0.291	-0.071
996	6.90503883	0.87	5.069	3.583	8.245	2.940	2.76553	5.36596	0.00000	7.710	0.000	0.664	0.334	0.002
1047	6.90905142	0.77	5.063	3.584	8.254	2.930	3.01319	5.64973	0.00000	7.923	0.000	0.603	0.399	-0.002
1071	6.91361523	0.66	5.057	3.585	8.264	2.929	3.26085	5.88192	0.00000	8.107	0.000	0.538	0.466	-0.004
1098	6.91809225	0.55	5.052	3.585	8.274	2.934	3.50851	6.06250	0.00000	8.300	0.000	0.475	0.530	-0.005
1134	6.92279530	0.44	5.048	3.586	8.287	2.947	3.67362	6.23019	0.00000	8.455	0.000	0.409	0.597	-0.006
1179	6.92745113	0.33	5.046	3.586	8.301	2.970	3.92128	6.34628	0.00000	8.571	0.000	0.346	0.661	-0.007
1236	6.93182802	0.23	5.049	3.586	8.317	3.000	4.08638	6.44302	0.00000	8.610	0.000	0.294	0.713	-0.006
1314	6.93659449	0.13	5.057	3.585	8.341	3.058	4.12250	6.53976	0.00000	8.494	0.000	0.250	0.755	-0.004
1491	6.94177723	0.02	5.090	3.582	8.400	3.224	4.11218	6.63650	0.00000	8.083	0.000	0.239	0.746	0.017

needed for a detailed test of the theory. As a final interesting point, Figure 9 reports the time behavior of the effective temperature for two looping supergiants with the same mass (16 $M_\odot$) but with a small difference in the adopted metallicity. It appears that the amount of metallicity is tuning the number ratio of red-to-blue supergiants, an occurrence which should be of great interest in modeling observational results.

4. DISCUSSION

Results in the previous section put in light a strong dependence of the He burning stellar structures on the amount of heavy elements. The problem of course arises about the origin of such a behavior. By looking at the literature on the argument, one finds that this scenario can be at least in part understood in the light of the exploratory study given by Tuchman & Wheeler (1989). Following these authors, it appears that for each given chemical composition, massive stars start burning He either on the Hayashi track or at much larger temperatures according to the size of the He core at the end of H burning. More precisely, one finds that for each given mass and for each given chemical composition there exists a critical core mass M^c_{He}. If $M^c_{He} < M_{He}$, the star ignites He on the Hayashi track, if $M_{He} > M^c_{He}$, the He-burning phase starts as a blue supergiant.

TABLE 1—*Continued*

20M-- Y=0.27-- Z=0.006														
nmd	logt	H/He	LogL	logTe	logTc	logϱc	Mcc	Mc_He	M_CO	Mce	Lpp	Lcno	L3α	Lgr
3	0.19924378	0.72	4.625	4.527	7.499	0.525	9.44202	0.00000	0.00000	0.000	0.000	1.000	0.000	0.000
42	3.83648491	0.72	4.671	4.554	7.543	0.669	5.72713	0.00000	0.00000	0.000	0.001	0.242	0.000	0.757
108	6.27932167	0.62	4.687	4.555	7.567	0.701	8.59069	0.00000	0.00000	0.000	0.001	1.002	0.000	-0.003
138	6.56008673	0.51	4.748	4.548	7.577	0.704	7.81676	0.00000	0.00000	0.000	0.001	1.002	0.000	-0.003
165	6.69834137	0.40	4.802	4.537	7.589	0.717	7.35239	0.00000	0.00000	0.000	0.000	1.003	0.000	-0.003
189	6.78220940	0.29	4.850	4.522	7.603	0.742	6.26888	0.00000	0.00000	8.900	0.000	1.004	0.000	-0.004
213	6.84037256	0.18	4.894	4.502	7.622	0.787	5.41755	0.00000	0.00000	8.900	0.000	1.004	0.000	-0.004
249	6.87483120	0.08	4.927	4.483	7.646	0.857	4.78809	0.00000	0.00000	8.900	0.000	1.004	0.000	-0.004
480	6.89803219	0.00	4.977	4.508	7.778	1.271	3.67362	0.00000	0.00000	8.900	0.000	0.816	0.000	0.184
498	6.89823580	0.99	4.988	4.517	7.829	1.486	0.45404	4.82936	0.00000	8.126	0.000	0.654	0.000	0.346
519	6.89852142	0.99	4.978	4.486	7.902	1.894	0.00000	4.64362	0.00000	5.108	0.000	1.193	0.000	-0.193
531	6.89870405	0.99	4.996	4.455	7.948	2.118	0.00000	4.64362	0.00000	5.108	0.000	1.166	0.000	-0.167
543	6.89888430	0.99	5.010	4.424	7.997	2.336	0.00000	4.54043	0.00000	5.087	0.000	1.146	0.000	-0.146
555	6.89905930	0.99	5.018	4.391	8.051	2.542	0.00000	4.54043	0.00000	5.067	0.000	1.126	0.000	-0.126
564	6.89918947	0.99	5.022	4.364	8.094	2.689	0.00000	4.54043	0.00000	5.067	0.000	1.106	0.000	-0.106
573	6.89930868	0.99	5.024	4.336	8.134	2.820	0.00000	4.54043	0.00000	5.087	0.000	1.082	0.000	-0.082
582	6.89941788	0.99	5.026	4.309	8.173	2.929	0.03096	4.64362	0.00000	5.276	0.000	1.056	0.009	-0.065
603	6.89951801	0.99	5.026	4.280	8.206	2.997	0.55723	4.64362	0.00000	5.598	0.000	1.005	0.090	-0.095
615	6.89961863	0.99	5.025	4.249	8.224	3.013	1.27957	4.64362	0.00000	5.805	0.000	0.962	0.238	-0.200
624	6.89970779	0.99	5.024	4.221	8.229	3.008	1.60979	4.74681	0.00000	6.385	0 000	0.941	0.290	-0.231
633	6.89979219	0.99	5.022	4.192	8.232	3.000	1.85745	4.74681	0.00000	7.352	0.000	0.939	0.299	-0.238
642	6.89986801	0.98	5.021	4.162	8.233	2.994	2.02255	4.74681	0.00000	7.314	0.000	0.936	0.306	-0.242
651	6.89993906	0.98	5.021	4.132	8.234	2.988	2.10511	4.82936	0.00000	7.314	0.000	0.933	0.302	-0.234
660	6.90000629	0.98	5.020	4.101	8.234	2.984	2.18766	4.82936	0.00000	8.591	0.000	0.928	0.302	-0.230
669	6.90006876	0.98	5.018	4.069	8.234	2.981	2.27021	4.82936	0.00000	8.591	0.000	0.925	0.301	-0.225
678	6.90012693	0.98	5.017	4.036	8.234	2.978	2.27021	4.82936	0.00000	8.900	0.000	0.918	0.301	-0.219
687	6.90018082	0.98	5.016	4.002	8.235	2.976	2.27021	4.83968	0.00000	10.061	0.000	0.912	0.301	-0.213
696	6.90023088	0.97	5.016	3.967	8.235	2.975	2.27021	4.86032	0.00000	8.900	0.000	0.905	0.302	-0.207
702	6.90026236	0.97	5.015	3.942	8.235	2.974	2.35277	4.86032	0.00000	8.900	0.000	0.901	0.303	-0.204
711	6.90030766	0.97	5.014	3.905	8.235	2.972	2.35277	4.87064	0.00000	0.000	0.000	0.894	0.305	-0.199
720	6.90035057	0.97	5.012	3.868	8.235	2.971	2.35277	4.89128	0.00000	0.000	0.000	0.892	0.304	-0.196
729	6.90039015	0.97	5.008	3.831	8.235	2.970	2.35277	4.89128	0.00000	0.000	0.000	0.893	0.308	-0.201
735	6.90041399	0.97	5.005	3.806	8.235	2.970	2.35277	4.90160	0.00000	0.000	0.000	0.896	0.312	-0.208
741	6.90043688	0.97	5.000	3.780	8.235	2.970	2.35277	4.90160	0.00000	0.000	0.000	0.901	0.316	-0.217
750	6.90046740	0.97	4.991	3.742	8.236	2.969	2.35277	4.91191	0.00000	0.000	0.000	0.914	0.324	-0.238
756	6.90048599	0.97	4.982	3.717	8.236	2.969	2.35277	4.91191	0.00000	0.000	0.000	0.927	0.331	-0.259
765	6.90050983	0.97	4.966	3.682	8.236	2.968	2.35277	4.91191	0.00000	0.000	0.000	0.957	0.345	-0.302
774	6.90053034	0.97	4.944	3.655	8.236	2.968	2.35277	4.93255	0.00000	0.000	0.000	1.000	0.364	-0.364
795	6.90056658	0.97	4.892	3.629	8.236	2.967	2.35277	4.93255	0.00000	19.013	0.000	1.111	0.411	-0.522
849	6.90062904	0.97	4.998	3.604	8.236	2.965	2.43532	4.99447	0.00000	9.636	0.000	0.847	0.338	-0.184
957	6.90431547	0.87	5.070	3.598	8.246	2.939	2.76553	5.36596	0.00000	8.494	0.000	0.661	0.337	0.002
1002	6.90850973	0.77	5.066	3.599	8.253	2.924	3.09574	5.67553	0.00000	8.842	0.000	0.599	0.408	-0.007
1023	6.91299391	0.66	5.063	3.600	8.264	2.924	3.26085	5.90771	0.00000	9.249	0.000	0.541	0.455	0.005
1044	6.91709232	0.56	5.062	3.600	8.274	2.932	3.50851	6.08830	0.00000	9.481	0.000	0.484	0.521	-0.005
1074	6.92170334	0.45	5.062	3.600	8.286	2.942	3.75617	6.23019	0.00000	9.790	0.000	0.425	0.580	-0.005
1119	6.92682838	0.34	5.064	3.600	8.301	2.965	3.92128	6.38497	0.00000	9.958	0.000	0.363	0.644	-0.007
1170	6.93116188	0.24	5.068	3.600	8.316	2.993	4.08638	6.50106	0.00000	9.868	0.000	0.315	0.692	-0.006
1257	6.93638229	0.13	5.078	3.599	8.342	3.053	4.15991	6.59781	0.00000	9.539	0.000	0.267	0.737	-0.004
1431	6.94145918	0.02	5.106	3.596	8.401	3.220	4.17281	6.69455	0.00000	8.852	0.000	0.249	0.738	0.015

It happens that our massive models lay just at the border of this critical mass. Adopting the Ledoux criterion, when $Z \gg 0.002$ the mass of the core after the exhaustion of central He is just below the quoted limit M^c_{He}, so that the stars become red supergiants. On the contrary, the mixing allowed by the use of the Schwarzschild criterion at the border of the He core during the very final phase of central H exhaustion, makes the He core growing beyond the critical mass, thus igniting He as a blue supergiant. This occurrence has been supported by a suitable series of numerical experiments which convincingly disclosed that the behavior of the Schwarzschild models is the consequence of the small mixing of He at the border of the original He core.

As one should expect, the occurrence of blue or red He-burning structures appears to be related to the relative efficiency of the nuclear burnings. This is clearly shown by the time behavior of the efficiency of the various burning we report in Figure 10 for two models of 20 $M_\odot$ experiencing the blue loop, as compared to the behavior of a similar model but with the blue loop inhibited by a small extramixing around the core. One can easily recognize that the red supergiant is following a different solution with a larger efficiency of the central He

TABLE 1—*Continued*

2OM -- Y=0.25 -- Z=0.004

nmd	logt	H/He	logL	logTe	logTc	logϱc	Mcc	Mc_He	M_CO	Mce	Lpp	Lcno	L3α	Lgr
45	3.81354260	0.75	4.657	4.559	7.555	0.719	5.41755	0.00000	0.00000	0.000	0.001	0.266	0.000	0.732
111	6.29729700	0.65	4.665	4.557	7.574	0.733	8.59069	0.00000	0.00000	0.000	0.001	1.001	0.000	-0.003
141	6.58134651	0.54	4.726	4.551	7.584	0.737	7.66197	0.00000	0.00000	0.000	0.001	1.002	0.000	-0.003
165	6.70735788	0.44	4.774	4.541	7.595	0.747	7.04282	0.00000	0.00000	0.000	0.000	1.003	0.000	-0.003
189	6.79526234	0.32	4.822	4.527	7.608	0.769	6.26888	0.00000	0.00000	8.745	0.000	1.003	0.000	-0.004
213	6.85909462	0.20	4.869	4.507	7.626	0.811	5.41755	0.00000	0.00000	8.745	0.000	1.004	0.000	-0.004
243	6.89492846	0.10	4.903	4.489	7.648	0.873	4.78809	0.00000	0.00000	8.745	0.000	1.004	0.000	-0.004
390	6.92273569	0.00	4.942	4.492	7.733	1.131	4.17926	0.00000	0.00000	8.745	0.000	0.973	0.000	0.027
498	6.92405128	0.00	4.969	4.517	7.832	1.495	1.44468	0.00000	0.00000	8.745	0.000	0.643	0.000	0.357
501	6.92409039	0.99	4.969	4.517	7.846	1.571	0.59464	4.54043	0.00000	5.185	0.000	0.825	0.000	0.174
519	6.92434216	0.99	4.958	4.487	7.908	1.925	0.00000	4.54043	0.00000	5.005	0.000	1.201	0.000	-0.201
531	6.92452240	0.99	4.976	4.458	7.953	2.151	0.00000	4.43723	0.00000	5.005	0.000	1.173	0.000	-0.173
543	6.92470026	0.99	4.990	4.427	8.001	2.369	0.00000	4.43723	0.00000	4.964	0.000	1.153	0.000	-0.153
555	6.92487288	0.99	4.999	4.395	8.056	2.575	0.00000	4.43723	0.00000	4.943	0.000	1.134	0.000	-0.134
564	6.92500305	0.99	5.003	4.369	8.099	2.724	0.00000	4.43723	0.00000	4.943	0.000	1.115	0.000	-0.115
573	6.92512369	0.99	5.005	4.342	8.140	2.857	0.00000	4.43723	0.00000	4.964	0.000	1.092	0.001	-0.092
582	6.92523384	0.99	5.008	4.314	8.179	2.964	0.07481	4.43723	0.00000	5.172	0.000	1.061	0.013	-0.074
603	6.92532587	0.99	5.009	4.288	8.209	3.023	0.55062	4.54043	0.00000	5.392	0.000	1.008	0.103	-0.111
615	6.92543507	0.99	5.010	4.257	8.226	3.031	1.27055	4.54043	0.00000	5.701	0.000	0.959	0.252	-0.211
624	6.92552853	0.99	5.010	4.228	8.230	3.020	1.66654	4.55332	0.00000	6.230	0.000	0.936	0.291	-0.227
633	6.92561817	0.99	5.010	4.200	8.232	3.010	1.88389	4.64362	0.00000	6.385	0.000	0.930	0.297	-0.227
642	6.92570210	0.98	5.010	4.170	8.232	3.002	1.98837	4.64362	0.00000	7.004	0.000	0.925	0.291	-0.216
651	6.92578125	0.98	5.011	4.140	8.232	2.996	2.06899	4.64362	0.00000	8.745	0.000	0.916	0.288	-0.204
660	6.92585754	0.98	5.012	4.110	8.233	2.992	2.12059	4.66941	0.00000	8.745	0.000	0.906	0.286	-0.191
669	6.92593098	0.98	5.013	4.078	8.233	2.989	2.15154	4.69521	0.00000	8.745	0.000	0.895	0.284	-0.179
678	6.92600107	0.98	5.014	4.046	8.233	2.986	2.17218	4.74681	0.00000	8.745	0.000	0.883	0.283	-0.167
687	6.92606974	0.97	5.015	4.012	8.233	2.984	2.19282	4.74681	0.00000	0.000	0.000	0.872	0.283	-0.155
696	6.92613602	0.97	5.016	3.977	8.234	2.982	2.20314	4.74681	0.00000	0.000	0.000	0.861	0.282	-0.143
702	6.92617941	0.97	5.017	3.952	8.234	2.981	2.21346	4.75713	0.00000	0.000	0.000	0.854	0.282	-0.136
711	6.92624378	0.97	5.018	3.915	8.234	2.980	2.23410	4.76745	0.00000	0.000	0.000	0.845	0.283	-0.128
720	6.92630672	0.97	5.018	3.877	8.234	2.978	2.24441	4.78808	0.00000	0.000	0.000	0.838	0.285	-0.123
726	6.92634726	0.97	5.017	3.852	8.234	2.978	2.24441	4.82936	0.00000	0.000	0.000	0.835	0.286	-0.120
732	6.92638588	0.97	5.015	3.827	8.234	2.977	2.25473	4.82936	0.00000	0.000	0.000	0.833	0.288	-0.121
738	6.92642307	0.96	5.012	3.800	8.235	2.976	2.26505	4.82936	0.00000	0.000	0.000	0.834	0.291	-0.125
744	6.92645741	0.96	5.009	3.774	8.235	2.976	2.26505	4.82936	0.00000	0.000	0.000	0.836	0.293	-0.130
750	6.92648888	0.96	5.004	3.748	8.235	2.975	2.27537	4.82936	0.00000	0.000	0.000	0.841	0.298	-0.139
756	6.92651796	0.96	4.997	3.722	8.235	2.975	2.27537	4.82936	0.00000	0.000	0.000	0.850	0.303	-0.152
765	6.92655516	0.96	4.984	3.686	8.235	2.974	2.28569	4.82936	0.00000	0.000	0.000	0.871	0.314	-0.185
774	6.92658520	0.96	4.964	3.658	8.235	2.974	2.28569	4.82936	0.00000	0.000	0.000	0.905	0.328	-0.233
795	6.92663479	0.96	4.915	3.633	8.235	2.973	2.29601	4.85000	0.00000	18.961	0.000	0.996	0.369	-0.366
858	6.92673826	0.96	5.019	3.610	8.236	2.972	2.31665	4.85000	0.00000	9.326	0.000	0.763	0.295	-0.058
939	6.93063879	0.85	5.045	3.608	8.246	2.947	2.67782	5.26277	0.00000	9.403	0.000	0.655	0.344	0.001
972	6.93434048	0.75	5.042	3.609	8.254	2.939	2.93580	5.52074	0.00000	10.061	0.000	0.600	0.402	-0.002
990	6.93840504	0.65	5.041	3.610	8.263	2.937	3.18346	5.72713	0.00000	10.667	0.000	0.543	0.461	-0.004
1014	6.94292116	0.54	5.041	3.610	8.274	2.942	3.43112	5.93351	0.00000	11.299	0.000	0.482	0.525	-0.006
1041	6.94687939	0.44	5.042	3.611	8.285	2.953	3.62718	6.06250	0.00000	11.815	0.000	0.430	0.577	-0.007
1083	6.95158434	0.33	5.045	3.611	8.300	2.973	3.81293	6.21084	0.00000	12.022	0.000	0.373	0.631	-0.004
1137	6.95604992	0.23	5.050	3.610	8.317	3.008	3.99867	6.32693	0.00000	11.815	0.000	0.323	0.684	-0.006
1227	6.96117735	0.13	5.060	3.609	8.342	3.062	4.03995	6.42367	0.00000	11.093	0.000	0.274	0.731	-0.004
1401	6.96602201	0.02	5.084	3.606	8.400	3.229	4.06059	6.52041	0.00000	9.694	0.000	0.252	0.735	0.014

burning which is balanced by a lower efficiency of the H shell burning. Moreover, Figure 10 discloses that when the red supergiant model shifts to the blue, the interior burnings are exactly driven to the blue solution.

5. FINAL REMARKS

In this paper we explored the behavior of canonical models of massive stars. We found that the star metallicity is a critical parameter governing the occurrence of blue loops during the He burning phase. For $Z \geq 0.006$ all the supergiants more luminous than $M_{bol} \approx -6.5$ should be red. For $0.003 < Z < 0.006$ we can expect luminous He burning giants clumping in the two blue and red groups. Only for lower metallicity one expects He burning giants substantially confined at large effective temperatures.

At present, such a theoretical scenario appears not to be contradicted by very general observational constraints derived from the MC clusters NGC 2004 and NGC 330. Further investigations and, in particular, observational tests are needed before deriving final conclusions about the adopted evolution ary scenario. However, when this paper was already accom-

TABLE 1—*Continued*

20M -- Y=0.25 -- Z=0.003

nmd	logt	H/He	logL	logTe	logTc	logρc	Mcc	Mc_He	M_CO	Mce	Lpp	Lcno	L3α	Lgr.
42	3.71805811	0.75	4.655	4.561	7.555	0.720	5.21117	0.00000	0.00000	0.000	0.001	0.204	0.000	0.795
111	6.28539085	0.65	4.667	4.563	7.580	0.755	8.59069	0.00000	0.00000	0.000	0.001	1.001	0.000	-0.003
141	6.57584763	0.54	4.728	4.557	7.591	0.759	7.81676	0.00000	0.00000	0.000	0.001	1.002	0.000	-0.003
165	6.70397377	0.44	4.776	4.547	7.602	0.769	7.04282	0.00000	0.00000	8.591	0.001	1.003	0.000	-0.003
189	6.79261923	0.33	4.824	4.534	7.615	0.791	6.26888	0.00000	0.00000	8.591	0.000	1.003	0.000	-0.004
207	6.84360313	0.23	4.860	4.519	7.628	0.820	5.62394	0.00000	0.00000	8.591	0.000	1.004	0.000	-0.004
234	6.88599110	0.13	4.897	4.500	7.649	0.876	5.07702	0.00000	0.00000	8.591	0.000	1.004	0.000	-0.004
312	6.91660166	0.02	4.933	4.486	7.698	1.021	4.38564	0.00000	0.00000	8.591	0.000	1.000	0.000	0.000
456	6.92259884	0.00	4.955	4.511	7.777	1.273	3.83872	0.00000	0.00000	8.591	0.000	0.888	0.000	0.112
498	6.92298126	1.00	4.971	4.523	7.850	1.570	0.72234	4.64362	0.00000	5.418	0.000	0.746	0.000	0.254
552	6.92377138	1.00	5.002	4.406	8.058	2.575	0.00000	4.43723	0.00000	4.964	0.000	1.135	0.000	-0.135
570	6.92402935	1.00	5.009	4.354	8.143	2.862	0.00000	4.43723	0.00000	4.984	0.000	1.093	0.001	-0.094
579	6.92413473	1.00	5.012	4.329	8.180	2.963	0.08513	4.43723	0.00000	5.005	0.000	1.061	0.012	-0.073
612	6.92433977	0.99	5.016	4.274	8.227	3.032	1.28086	4.54043	0.00000	5.701	0.000	0.952	0.252	-0.204
630	6.92453814	0.99	5.019	4.217	8.232	3.008	1.90388	4.64362	0.00000	6.540	0.000	0.917	0.293	-0.210
639	6.92463255	0.98	5.020	4.188	8.233	2.999	2.01739	4.64362	0.00000	7.507	0.000	0.908	0.287	-0.195
666	6.92489958	0.98	5.026	4.098	8.233	2.985	2.16186	4.74681	0.00000	8.591	0.000	0.867	0.276	-0.144
675	6.92498732	0.97	5.029	4.065	8.234	2.982	2.19282	4.74681	0.00000	8.591	0.000	0.852	0.276	-0.128
684	6.92507744	0.97	5.032	4.032	8.234	2.980	2.21346	4.76745	0.00000	0.000	0.000	0.836	0.275	-0.112
693	6.92516994	0.97	5.034	3.997	8.234	2.978	2.23410	4.82936	0.00000	0.000	0.000	0.823	0.275	-0.097
702	6.92526531	0.97	5.036	3.961	8.235	2.976	2.24441	4.82936	0.00000	0.000	0.000	0.809	0.275	-0.084
723	6.92550325	0.96	5.039	3.872	8.235	2.972	2.28569	4.85000	0.00000	0.000	0.000	0.784	0.278	-0.063
735	6.92564440	0.96	5.038	3.820	8.236	2.970	2.30633	4.87064	0.00000	0.000	0.000	0.776	0.282	-0.058
741	6.92571259	0.95	5.036	3.793	8.236	2.969	2.31665	4.87064	0.00000	0.000	0.000	0.774	0.284	-0.057
759	6.92588663	0.95	5.023	3.711	8.237	2.967	2.33729	4.91191	0.00000	0.000	0.000	0.783	0.297	-0.080
768	6.92594814	0.95	5.010	3.676	8.237	2.967	2.34761	4.91191	0.00000	0.000	0.000	0.801	0.308	-0.109
825	6.92611456	0.94	4.960	3.622	8.237	2.965	2.36824	4.93255	0.00000	13.879	0.000	0.863	0.351	-0.215
921	6.92988300	0.84	5.042	3.614	8.247	2.944	2.70878	5.31436	0.00000	10.164	0.000	0.645	0.353	0.002
954	6.93427038	0.73	5.039	3.615	8.257	2.936	3.00803	5.59814	0.00000	11.403	0.000	0.580	0.423	-0.003
972	6.93823719	0.62	5.039	3.617	8.266	2.938	3.23505	5.77872	0.00000	12.538	0.000	0.525	0.479	-0.003
1071	6.94517231	0.45	5.107	3.645	8.284	2.952	3.59622	6.03670	0.00000	0.000	0.000	0.396	0.488	0.117
1125	6.94528151	0.45	5.128	3.789	8.285	2.952	3.59622	6.06250	0.00000	0.000	0.000	0.396	0.466	0.137
1137	6.94532728	0.45	5.128	3.852	8.285	2.953	3.59622	6.06250	0.00000	0.000	0.000	0.405	0.467	0.128
1143	6.94535732	0.45	5.127	3.885	8.285	2.953	3.59622	6.06250	0.00000	0.000	0.000	0.411	0.468	0.121
1155	6.94543743	0.44	5.123	3.960	8.285	2.953	3.59622	6.06250	0.00000	0.000	0.000	0.426	0.472	0.102
1173	6.94566679	0.44	5.113	4.073	8.286	2.955	3.58590	6.08830	0.00000	0.000	0.000	0.459	0.486	0.056
1179	6.94582462	0.43	5.107	4.108	8.287	2.956	3.58590	6.08830	0.00000	0.000	0.000	0.472	0.494	0.034
1185	6.94616079	0.42	5.101	4.139	8.288	2.958	3.60654	6.08830	0.00000	0.000	0.000	0.484	0.506	0.010
1224	6.95041037	0.32	5.102	4.164	8.301	2.974	3.83356	6.24953	0.00000	9.268	0.000	0.444	0.564	-0.007
1293	6.95586157	0.21	5.107	4.161	8.321	3.011	4.00899	6.42367	0.00000	9.268	0.000	0.384	0.620	-0.004
1383	6.96060848	0.13	5.111	4.134	8.341	3.052	4.30583	6.55911	0.00000	0.000	0.000	0.312	0.791	-0.102
1461	6.96363449	0.08	5.113	4.107	8.364	3.111	4.13314	6.65585	0.00000	0.000	0.000	0.298	0.708	-0.006
1494	6.96457052	0.06	5.113	4.082	8.376	3.144	4.14669	6.65585	0.00000	0.000	0.000	0.288	0.719	-0.005
1524	6.96525860	0.04	5.112	4.056	8.386	3.174	4.15910	6.67520	0.00000	0.000	0.000	0.280	0.726	-0.005
1611	6.96655273	0.02	5.107	3.952	8.415	3.260	4.15910	6.69455	0.00000	0.000	0.000	0.267	0.737	-0.002
1629	6.96671915	0.01	5.105	3.925	8.420	3.277	4.15910	6.71390	0.00000	0.000	0.000	0.266	0.737	-0.001
1680	6.96706247	0.01	5.097	3.843	8.435	3.322	4.14669	6.71390	0.00000	0.000	0.000	0.266	0.734	0.002
1710	6.96719837	0.01	5.089	3.785	8.443	3.346	4.14669	6.71390	0.00000	0.000	0.000	0.269	0.732	0.002
1722	6.96724272	0.01	5.084	3.760	8.446	3.356	4.13314	6.71390	0.00000	0.000	0.000	0.271	0.732	0.001
1746	6.96731758	0.00	5.070	3.706	8.452	3.374	4.11960	6.71390	0.00000	0.000	0.000	0.278	0.737	-0.011
1773	6.96738338	0.00	5.035	3.653	8.458	3.393	4.10605	6.71390	0.00000	0.000	0.000	0.298	0.769	-0.063

plished, we got knowledge of a very recent work by Stothers & Chin (1992), who presented a careful investigation of the evolutionary behavior of stars in the 3–15 $M_{\odot}$ range. Comparison with observation of supergiants in NGC 330 and NGC 458 derive the quoted A's to conclusions which largely support the present analysis. This gives us hope that we may be on the right road.

It is a pleasure to thank R. Stothers and C. W. Chin for making available their work before publication.

TABLE 1—*Continued*

20M -- Y=0.25-- Z=0.002

nmd	logt	H/He	logL	logTe	logTc	logρc	Mcc	Mc_He	M_CO	Mce	Lpp	Lcno	L3α	Lgr
45	3.73697352	0.75	4.665	4.573	7.573	0.775	5.41755	0.00000	0.00000	0.000	0.002	0.276	0.000	0.722
111	6.28916025	0.65	4.671	4.571	7.591	0.785	8.74548	0.00000	0.00000	0.000	0.002	1.001	0.000	-0.003
141	6.57608318	0.54	4.732	4.565	7.601	0.789	7.81676	0.00000	0.00000	0.000	0.001	1.002	0.000	-0.003
165	6.70408392	0.44	4.780	4.556	7.612	0.799	7.04282	0.00000	0.00000	0.000	0.001	1.003	0.000	-0.003
189	6.79210377	0.33	4.828	4.542	7.625	0.821	6.26888	0.00000	0.00000	8.745	0.000	1.003	0.000	-0.004
210	6.85008192	0.22	4.870	4.525	7.641	0.856	5.62394	0.00000	0.00000	8.745	0.000	1.004	0.000	-0.004
237	6.88858318	0.12	4.905	4.506	7.662	0.912	4.91191	0.00000	0.00000	8.745	0.000	1.004	0.000	-0.005
312	6.91659260	0.02	4.938	4.495	7.709	1.052	4.38564	0.00000	0.00000	8.745	0.000	1.000	0.000	0.000
456	6.92256117	0.00	4.960	4.520	7.789	1.309	3.83872	0.00000	0.00000	8.745	0.000	0.883	0.000	0.117
495	6.92291927	1.00	4.976	4.532	7.857	1.579	1.01128	4.64362	0.00000	8.745	0.000	0.666	0.000	0.333
516	6.92321348	1.00	4.967	4.501	7.929	1.986	0.00000	4.54043	0.00000	5.025	0.000	1.189	0.000	-0.189
552	6.92375851	1.00	5.009	4.412	8.078	2.634	0.00000	4.43723	0.00000	5.005	0.000	1.128	0.000	-0.128
561	6.92389297	1.00	5.014	4.387	8.121	2.783	0.00000	4.43723	0.00000	5.005	0.000	1.107	0.000	-0.108
588	6.92413330	1.00	5.022	4.332	8.202	3.006	0.35270	4.54043	0.00000	5.067	0.000	1.024	0.053	-0.076
603	6.92424011	0.99	5.025	4.305	8.225	3.032	1.06956	4.54043	0.00000	5.598	0.000	0.961	0.211	-0.172
621	6.92446089	0.99	5.031	4.250	8.233	3.006	1.89356	4.64362	0.00000	6.540	0.000	0.902	0.289	-0.191
630	6.92457199	0.98	5.033	4.222	8.233	2.996	2.03545	4.66941	0.00000	6.695	0.000	0.890	0.282	-0.172
639	6.92468262	0.98	5.036	4.193	8.233	2.989	2.11027	4.74681	0.00000	7.662	0.000	0.874	0.276	-0.150
648	6.92479467	0.98	5.041	4.164	8.234	2.983	2.16186	4.74681	0.00000	8.745	0.000	0.854	0.272	-0.126
657	6.92491245	0.97	5.045	4.134	8.234	2.980	2.19282	4.76745	0.00000	8.745	0.000	0.834	0.269	-0.103
666	6.92504025	0.97	5.050	4.103	8.234	2.976	2.22378	4.82936	0.00000	8.745	0.000	0.814	0.268	-0.081
675	6.92518520	0.97	5.055	4.071	8.235	2.973	2.25473	4.82936	0.00000	0.000	0.000	0.792	0.267	-0.060
684	6.92536449	0.96	5.060	4.038	8.235	2.970	2.28569	4.87064	0.00000	0.000	0.000	0.771	0.267	-0.038
693	6.92561960	0.96	5.066	4.003	8.236	2.967	2.31665	4.91191	0.00000	0.000	0.000	0.748	0.269	-0.017
711	6.92712355	0.91	5.080	4.003	8.241	2.953	2.49207	5.09766	0.00000	0.000	0.000	0.700	0.287	0.013
729	6.92871284	0.87	5.085	4.063	8.245	2.945	2.63912	5.26277	0.00000	0.000	0.000	0.681	0.310	0.009
738	6.92979765	0.84	5.087	4.091	8.247	2.941	2.71652	5.36596	0.00000	0.000	0.000	0.668	0.325	0.007
756	6.93359709	0.74	5.093	4.153	8.256	2.933	2.97707	5.62394	0.00000	0.000	0.000	0.624	0.375	0.001
768	6.93645477	0.66	5.097	4.180	8.263	2.931	3.17314	5.80452	0.00000	0.000	0.000	0.590	0.410	0.000
789	6.94052744	0.56	5.103	4.206	8.273	2.934	3.42080	6.01090	0.00000	0.000	0.000	0.543	0.460	-0.002
819	6.94502974	0.45	5.108	4.223	8.286	2.945	3.67878	6.21084	0.00000	9.829	0.000	0.491	0.513	-0.004
858	6.94946909	0.34	5.113	4.231	8.299	2.962	3.90580	6.38497	0.00000	10.061	0.000	0.440	0.565	-0.005
912	6.95403624	0.24	5.117	4.229	8.315	2.989	4.13411	6.50106	0.00000	0.000	0.000	0.387	0.622	-0.008
999	6.95914316	0.13	5.122	4.204	8.342	3.050	4.28164	6.65585	0.00000	9.829	0.000	0.335	0.673	-0.008
1059	6.96175337	0.10	5.125	4.179	8.354	3.076	4.19860	6.71390	0.00000	0.000	0.000	0.312	0.697	-0.008
1101	6.96315145	0.07	5.126	4.153	8.369	3.118	4.22440	6.73324	0.00000	0.000	0.000	0.296	0.711	-0.007
1140	6.96414948	0.05	5.126	4.127	8.383	3.157	4.23649	6.77194	0.00000	0.000	0.000	0.286	0.720	-0.005
1176	6.96485329	0.03	5.126	4.100	8.395	3.193	4.24778	6.77194	0.00000	0.000	0.000	0.279	0.725	-0.003
1236	6.96565294	0.02	5.125	4.049	8.414	3.251	4.23649	6.79129	0.00000	0.000	0.000	0.273	0.726	0.002
1266	6.96591806	0.01	5.124	4.023	8.423	3.279	4.23649	6.81064	0.00000	0.000	0.000	0.273	0.723	0.007
1296	6.96611786	0.01	5.122	3.996	8.432	3.305	4.22440	6.81064	0.00000	0.000	0.000	0.273	0.716	0.013
1353	6.96636963	0.01	5.118	3.944	8.447	3.351	4.19860	6.81064	0.00000	0.000	0.000	0.277	0.691	0.036
1383	6.96645594	0.00	5.116	3.919	8.454	3.374	4.18570	6.81064	0.00000	0.000	0.000	0.280	0.669	0.054
1464	6.96659851	0.00	5.109	3.866	8.471	3.427	4.03995	6.81064	0.00000	0.000	0.000	0.292	0.580	0.132
1512	6.96664572	0.00	5.105	3.840	8.480	3.454	3.84388	6.81064	0.00000	0.000	0.000	0.300	0.506	0.199
1575	6.96672106	0.00	5.094	3.787	8.502	3.521	2.93161	6.81064	0.00000	0.000	0.000	0.326	0.207	0.474
1593	6.96675158	0.00	5.087	3.758	8.516	3.566	1.97841	6.81064	0.00000	0.000	0.000	0.344	0.035	0.631
1611	6.96678448	0.00	5.075	3.724	8.533	3.621	0.00000	6.81064	4.53398	0.299	0.000	0.360	0.011	0.642
1674	6.96685505	0.00	4.995	3.646	8.567	3.732	0.00000	6.81064	4.53398	0.000	0.000	0.395	0.075	0.555
1722	6.96692514	0.00	5.077	3.619	8.596	3.839	0.00000	6.81064	4.53398	9.984	0.000	0.290	0.311	0.432
1755	6.96708393	0.00	5.179	3.611	8.639	4.016	0.00000	6.81064	4.53398	8.310	0.000	0.138	0.735	0.178

NOTES.—Selected physical quantities describing the evolution of our 20 $M_{\odot}$ models for the various labeled assumptions about the star composition. *Left to right:* sequence number of the model (nmd), age t (in yr), central abundance of H or He, star luminosity (in solar units), effective temperature, central temperature and density, mass (in solar units) of the convective core (M_{cc}), of the central He core ($M_{c_{He}}$) and of the carbon-oxygen core (M_{CO}), mass location of the bottom of the convective envelope (M_{ce}), luminosity originated by *pp*, CNO, 3α burnings and gravitation, all in units of the stellar luminosity.

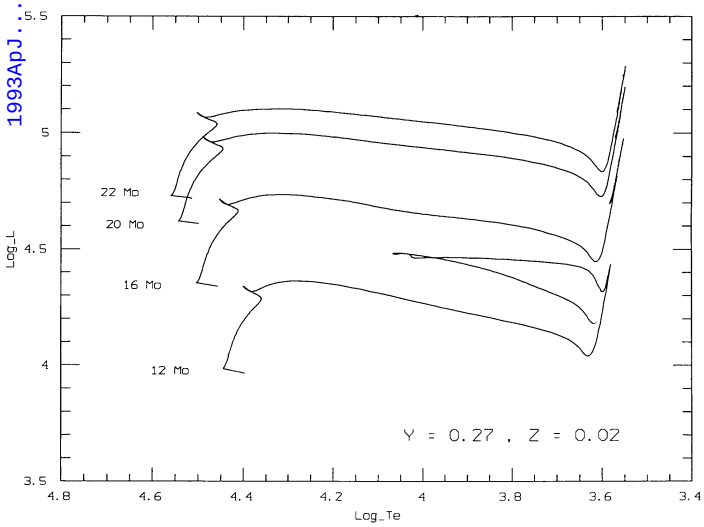

FIG. 2.—Evolutionary path of our massive models for $Y = 0.27, Z = 0.02$

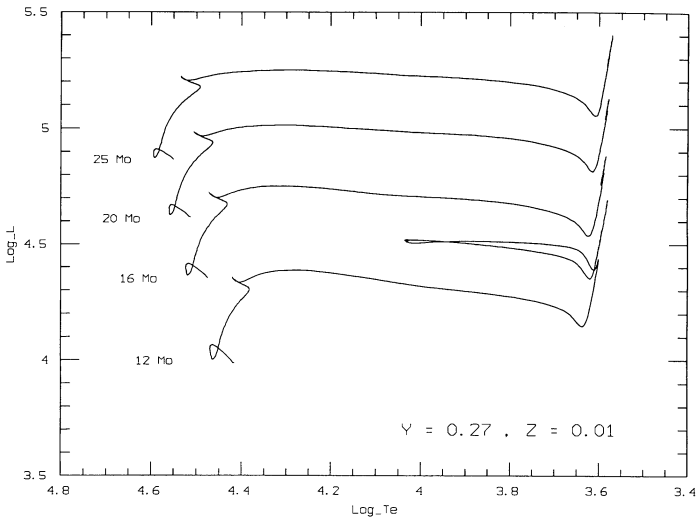

FIG. 3.—Same as in Fig. 2 but for $Y = 0.27, Z = 0.01$

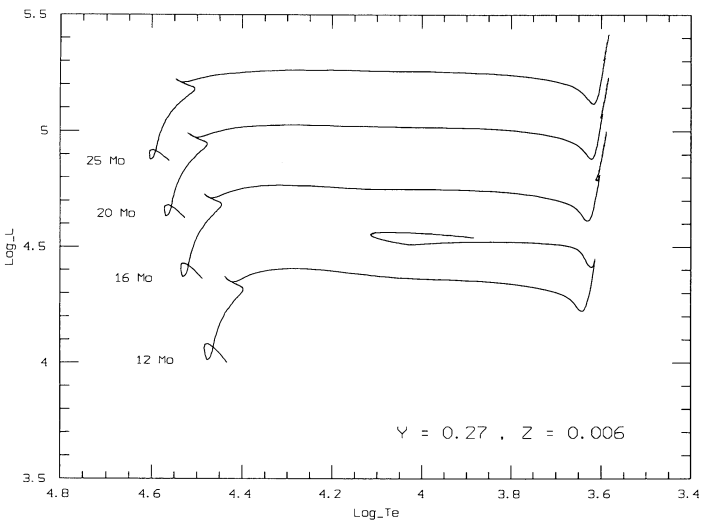

FIG. 4.—Same as in Fig. 2 but for $Y = 0.27, Z = 0.06$

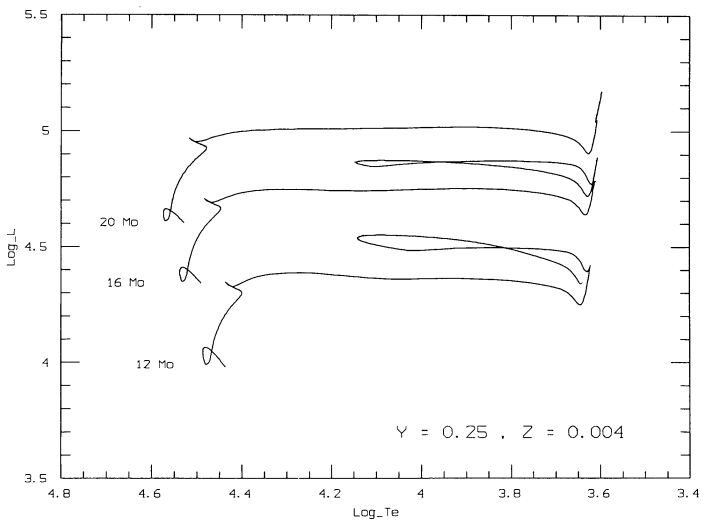

FIG. 5.—Same as Fig. 2 but for $Y = 0.25, Z = 0.004$

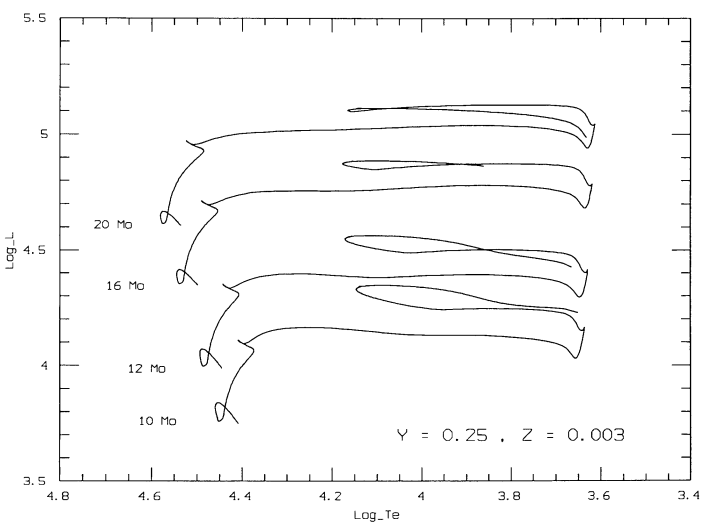

FIG. 6.—Same as in Fig. 2 but for $Y = 0.25, Z = 0.003$

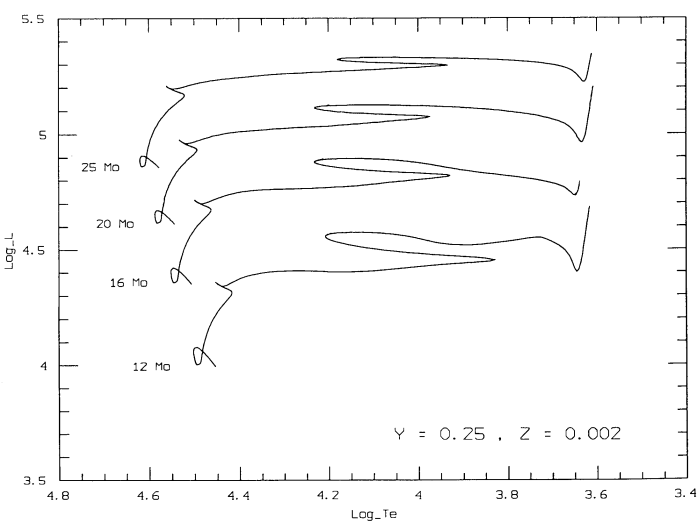

FIG. 7.—Same as in Fig. 2 but for $Y = 0.25, Z = 0.002$

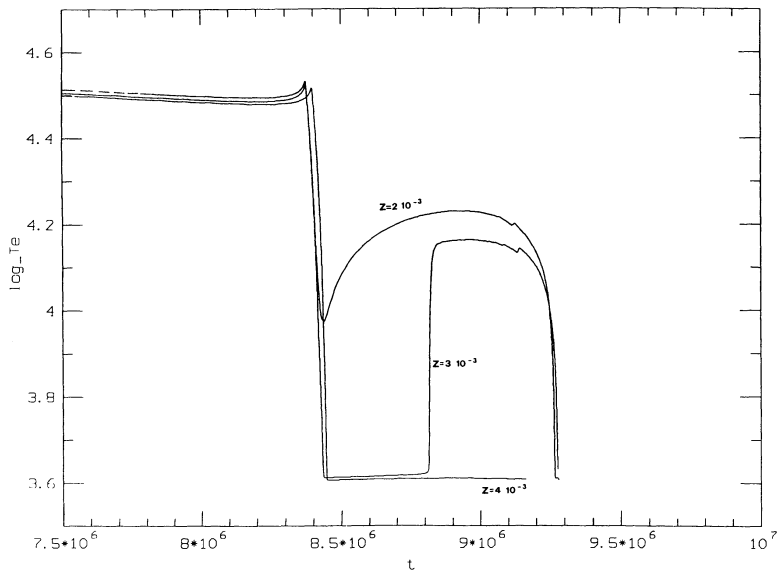

FIG. 8.—Time behavior of the effective temperature of selected 20 $M_{\odot}$ models for the labeled assumptions on the star metallicity

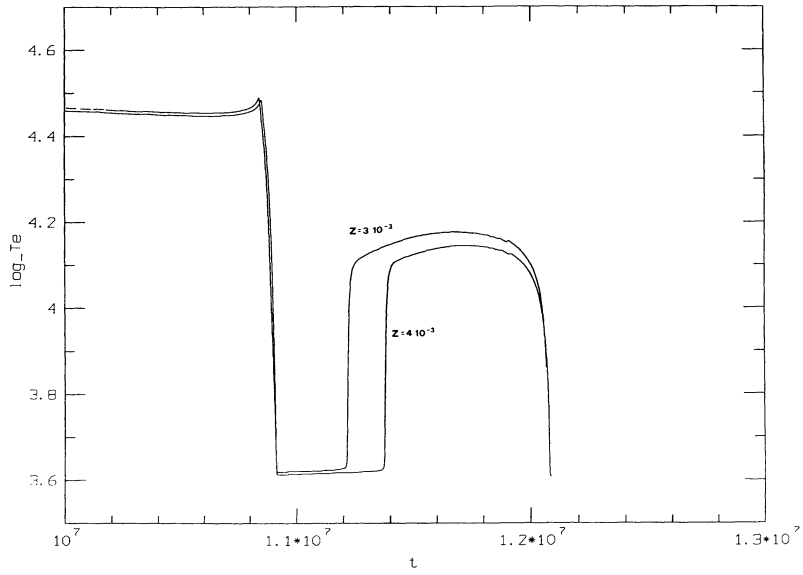

FIG. 9.—Red to blue ratio as a function of star metallicity

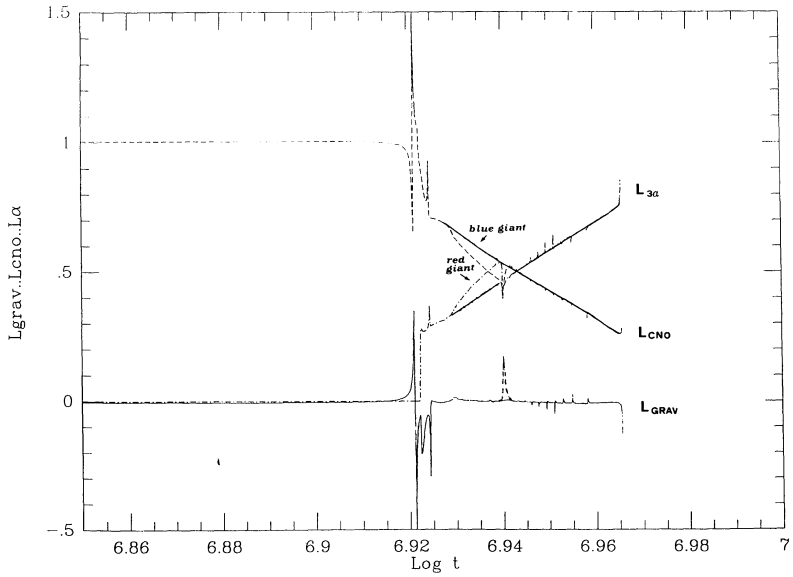

FIG. 10.—Time behavior of the production of energy in the supergiant igniting He to the blue (*full lines*) compared with the same behavior for a supergiant making the blue loop (*dashed lines*).

REFERENCES

Alcock, C., & Paczyński, B. 1978, ApJ, 223, 244
Bencivenni, D., Brocato, E., Buonanno, R., & Castellani, V. 1991, AJ, 102, 137
Carney, B. W., Janes, K. A., & Flower, P. J. 1985, AJ, 90, 1196
Cassisi, S., Castellani, V., & Straniero, O. 1993, in preparation
Castellani, V., Chieffi, A., & Straniero, O. 1990, ApJS, 74, 463
———. 1992, ApJS, 78, 517
Cayrel, R. 1988, ESO Messenger, 54, 12
Chiosi, C. 1981, in Physical Processes in Red Giants, ed. I. Iben & A. Renzini (Dordrecht: Reidel), 183
Chiosi, C., & Maeder, A. 1986, ARA&A, 24, 329
Iben, I., Jr. 1974, ARA&A, 12, 215
Iglesias, C. A., & Roger, F. J. 1991a, ApJ, 371, 408
———. 1991b, ApJ, 371, L73
Maeder, A. 1990, A&AS, 84, 139
Roger, F. J., & Iglesias, C. A. 1992, ApJS, 152, 225
Stothers, R. B. 1991, ApJ, 383, 820
Stothers, R. B., & Chin, C.-W. 1968, ApJ, 152, 225
———. 1992, ApJ, 390, 136
Tuchman, Y., & Wheeler, J. C. 1989, ApJ, 344, 835
Weiss, A. 1989, ApJ, 339, 365